Transportation Research Part D 104 (2022) 103189

Contents lists available at ScienceDirect

Transportation Research Part D

journal homepage: www.elsevier.com/locate/trd

Land-Use microsimulation model for livelihood diversification after the 2010 Merapi volcano eruptions

Martin Garcia-Fry [a,*], Osamu Murao [b], Syamsul Bachri [c], Luis A. Moya [d]

[a] Department of Architecture and Building Science, Graduate School of Engineering, Tohoku University, Sendai, Japan
[b] International Research Institute of Disaster Science, Tohoku University, 468-1 Aramaki-Aza, Aoba-Ku, Sendai, Japan
[c] Department of Geography, Faculty of Social Science, State University of Malang, Jl. Semarang No.5, Sumbersari, Kec. Lowokwaru, Kota Malang, Jawa Timur, 65145 Malang, Indonesia
[d] Japan-Peru Center for Earthquake Engineering Research and Disaster Mitigation, National University of Engineering, Tupac Amaru Avenue, 1150 Lima, Peru

ARTICLE INFO

Keywords:
Recovery
Mobility
Accessibility
Rural Studies
Peri-Urban Networks

ABSTRACT

The 2010 Merapi Volcano eruptions caused significant damage in the Sleman Regency of Yogyakarta, Indonesia. Several households (HHs) were relocated to safely designated areas, but to sustain their livelihoods they have to travel back to their farmlands or change their identities as farmers. This study evaluates post-disaster mobility, aiming to clarify whether a land-use network with distributed livelihood options can complement rural labor in a recovery scenario. We collected sociodemographic and travel routine data in the affected areas. Then, the operational land use and transport microsimulation (OLUTM) model was performed to forecast a future scenario and gauge livelihood changes. Middle-aged farmers with upper median incomes and risk-taking behaviors were found to venture home businesses that contribute to rural labor. A 63% share of livelihoods diversified by farmers and 30% travel utility savings rendered a robust microsimulation system.

1. Introduction

On Tuesday, October 26, 2010, Indonesia's most active stratovolcano erupted thrice, forcing the evacuation of 400,000 people and destroying 2,847 homes (Maly et al. 2015; World Bank 2012). In response, the government relocated 2,608 households (HHs) on 23 resettlement sites in the Cangkringan district, Sleman Regency, Yogyakarta, Indonesia (World Bank 2016). The affected livelihoods were centered on dairy farming and agriculture, while tourism was the secondary employment with the standard minimum wages (Rindrasih 2018). As a result, people's recovery relied on daily trips to farmlands, dairy cooperatives, and tourist destinations.

HHs of the largest resettlement site, Pagerjurang, collectively believe that resettling has granted them safety from the volcano. However, resilience did not translate into secured livelihoods: (1) even though tourism became a main source of livelihood diversification, it failed to promote choices of livelihood in ample spheres of life; (2) middle-aged farmers and the elderly (48% of the active economic population) ([Dataset 2] Indonesia 2020) are "too tired from the daily grind of commuting to the dairy cooperative and their land on Mt. Merapi" (Miller M.A., 2018, p.202); and, (3) Yogyakarta's rural urbanization is shifting land-use structures that generate

* Corresponding author at: Room S402, Building J31, 468–1 Aramaki–Aza, Aoba–Ku, Sendai-Shi, Miyagi-Ken, Japan.
E-mail addresses: garcia.fry.martin.p2@dc.tohoku.ac.jp (M. Garcia-Fry), murao@irides.tohoku.ac.jp (O. Murao), syamsul.bachri.fis@um.ac.id (S. Bachri), lmoyah@uni.pe (L.A. Moya).

https://doi.org/10.1016/j.trd.2022.103189

Available online 9 February 2022

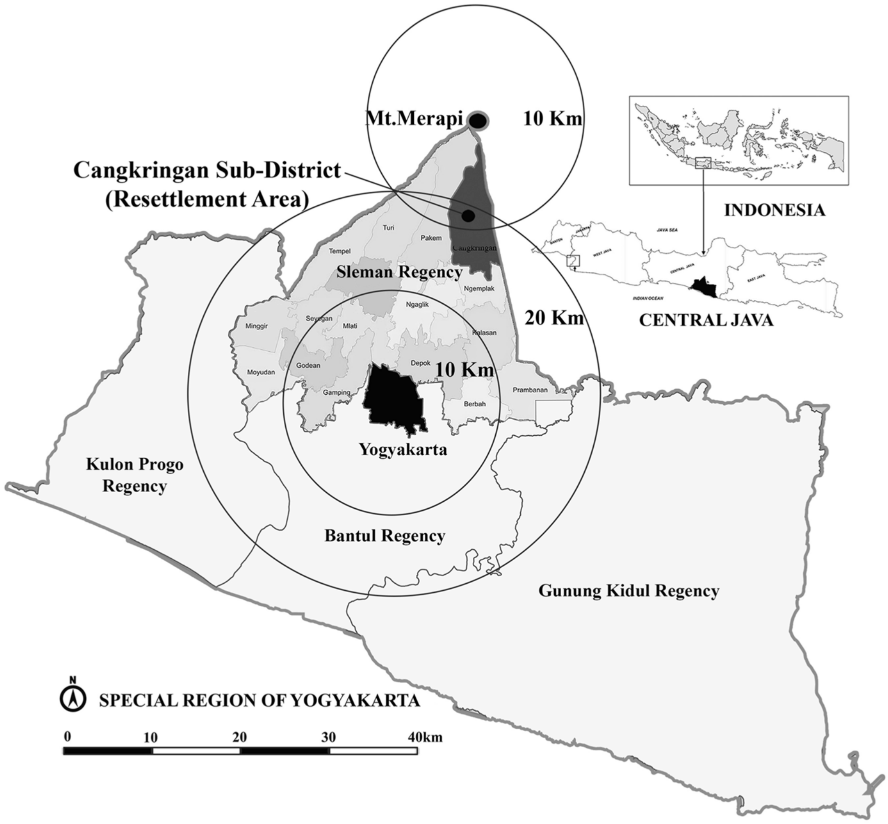

Fig. 1. Study area in the Special Region of Yogyakarta. Suburban areas of the city extend through all four regencies reaching 20 km distances from the center. The Cangkringan sub-district is home to 75% of the relocated HHs, previously living within 10 kms from Mt. Merapi's summit. (Gray, 1.5 columns).

place-attachment. As a result, identity loss is at stake, risking tourist-attractive value (Umaya et al. 2020). Therefore, how can we attract livelihood options closer to HHs while sustaining agricultural areas in the rural periphery of urban centers?

This paper describes our recent efforts to develop a sequential land use/transport model to evaluate post-disaster mobility and clarify whether a land-use network with distributed livelihood options can complement rural labor in a recovery scenario. The operational land use and transport microsimulation (OLUTM) model delivers a predictive network of land-use change. The method establishes key driving factors of a city's mobility system and applies them to rural areas. Then, through behavioral and urban form analysis, the outcome is evaluated through land use and travel simulations to explain that mobility with livelihood changes.

Specific contributions are: first, a significant probability of residential to mixed land-use change was found for middle-aged farmers with risk-taking lifestyles and upper median incomes venturing home-business entrepreneurships (HBEs). HBEs diversify livelihoods with non-farm activities that capitalize on local products and complement rural labor. Second, a land-use treatment in nodes incited land-use conversion between the nodes. This is not common in land-use modeling research because it targets HBEs in an agronomic-centric network.

In the following chapter, transportation planning is shown to be a channel of development consistent with the needs of disaster-affected areas. Chapter 3 introduces the study area and our method. Chapter 4 and Chapter 5 describe and perform sub-models of the OLUTM model, leading to an evaluation in Chapter 6 with findings and concluding remarks.

2. The influence of urban form on travel

Transportation and employment are important constituents of the urban form. Together, they can provide access to an equitable range of opportunities. Several meanings of accessibility exist (see Litman 2021), but this study follows the importance of reducing vehicle dependence as a factor of neighborhood accessibility (Krizek 2003). This means shorter distances in daily routines and having mobility choices for a variety of travel purposes. For instance, after the 2009 earthquake in L'Aquila, Italy, the isolation of houses made people dependent on private transport to access services, employment, or amenities (Contreras et al. 2017). In Yogyakarta, travel expenditures are not considered a burden because people adapted to the travel costs, lack of alternatives, and the perception that public transport is expensive (Herwangi et al. 2017).

While transport satisfies the need for mobility owing to the spatial separation of activities, urban form research examines physical

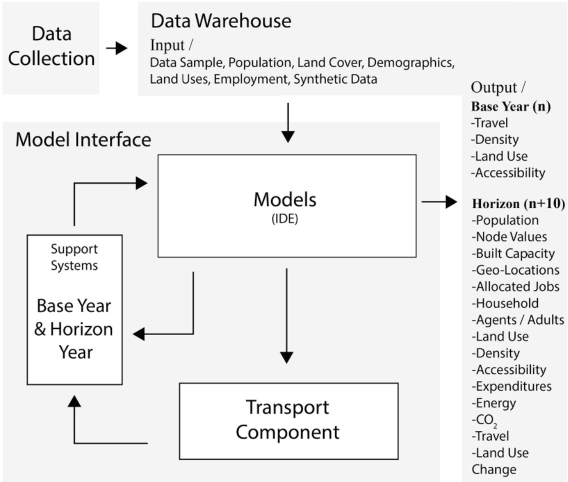

Fig. 2. Model architecture. (Gray, 1.5 columns).

characteristics that compose urban environments (size, shape, and the configuration of its parts) (Wegener and Fuerst 2004). For example, residents and firms want to be close to each other, saving on travel utilities and time. This causes economies of scale driven by agglomeration effects (Levinson and Wu 2020). These effects commonly expand in nodes of a transportation network, where local and inflowing resources meet profitably, creating building densities, activities, and people (Hynynen 2006). Nodes are defined by their scale of influence and employment shares in a traffic analysis zone (TAZ). TAZ's help to assign the expected growth and monitor trips in the network (Clifton et al. 2008).

In this paper, we evaluate development in a TAZ with three urban form measures: (i) density, defined by Handy et al. (2002) as the amount of population, employment, or building square-meters (m^2) per unit of area; (ii) land use, as the proximity of activities measured by the area of neighborhood shopping in a 400-meter radius, equivalent to a walking distance of 800 m, assumed by Yang and Diez-Roux (2012) to be a median distance for walking; and, (iii) accessibility, quantified by connectivity, road intersections, and block lengths (Krizek 2003).

2.1. *Model of microsimulation*

Land use and transport microsimulation models are modeling systems in which transportation and land use co-evolve over time (Miller E.J., 2018). The underlying concept is that development of the urban form and location of microdata (households, firms, agents, etc.) rely on accessibility to reach valued locations (Litman 2021). The OLUTM model follows the prospect theory, developed by Kahneman and Tversky (1979), to simulate random decisions based on the potential value of loss or gains in a two-stage decision-making process. The models here maximize the utility behavior of agents (people and vehicles) and objects (jobs, buildings, land uses, etc.) with sociodemographic data found by Kitamura (2009) to affect travel behavior.

While several influential studies have significantly advanced the computational barriers inherent to microscopic simulation (Miller and Salvini, 2005; Waddell et al. 2003; Wagner and Wegener 2007; Zhu et al. 2018; Zondag et al. 2015), they mainly derive findings from urban areas and do not address post-disaster mobility in rural areas. Moreover, similar realities exist (see Yokohari 2006; Bray 1994), but they were not meant to address urban growth.

3. Objective area and methodology

3.1. *The Cangkringan Sub-District*

Yogyakarta is the capital city of the Special Region of Yogyakarta (DIY), with a recorded population of 3,842,932 in 2019 ([Dataset 2] Indonesia 2020). The region is separated into four regency districts: Bantul, Kulon Progo, Sleman, Gunung Kidul, and Yogyakarta. Sleman is north of Yogyakarta, with Mt. Merapi at its northern apex surrounded by fertile agrarian land and the Cangkringan sub-district shown in Fig. 1.

The Sleman Regency has been facing rapid urbanization since before 2010, and is in need of better public service provision (Giyarsih 2010). A new spatial plan was adopted in 2012 called Rencana Tata Ruang Wilayah (RTRW) Kabupaten Sleman Tahun 2011–2031 as a top-down planning approach clarifying the distinction between urban and rural areas and regulating the scale and intensity of activities (Sleman Regency, 2012). Also, a law concerning sustainable agriculture food crops was issued by the Special Region of Yogyakarta in 2011, but urban expansion has continued to threaten food security in the region (Widowaty and Oktavian Artanto 2018).

There are three types of urban growth management initiatives imposed by governments worldwide: greenbelts (permanently limit

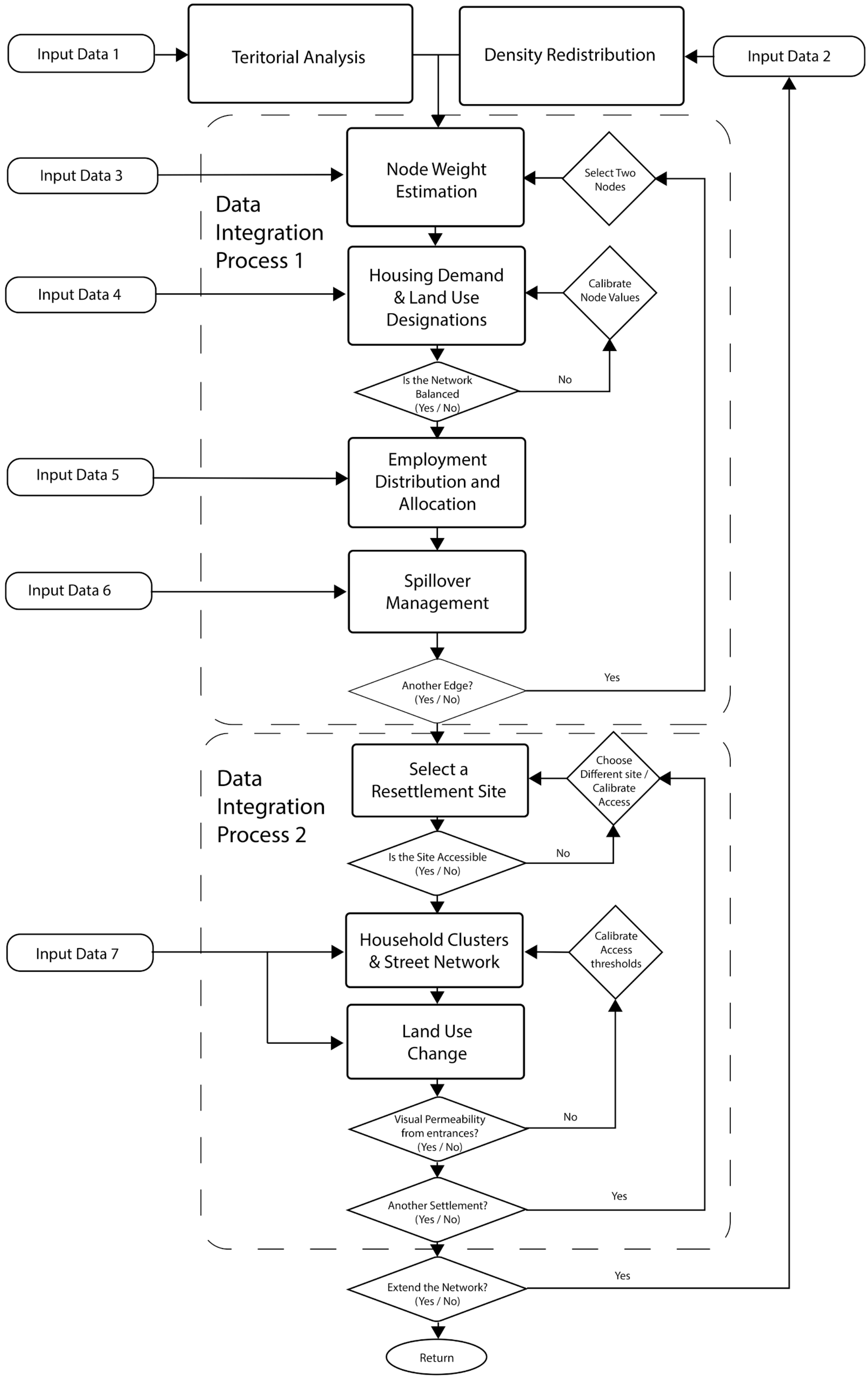

(caption on next page)

Fig. 3. Layout of the OLUTM model. Each iteration corresponds to one edge of the network. A future site-selection model is specified to locate resettlement sites in the second integration process. (B/W, 1.5 columns).

Table 1
Road network accessibility measures.

Categories		Connectivity		Intersections		Permeability	
Zone	**Building Density**	**Boundary Roads**	**Block Size (m)**	**Semi-Urban**	**Urban**	**Road Crossing**	**Level**
Residential	High	Local / Collector / Sub-Arterial	80 / 150 / 200	30 – 40	40 – 50	0	Zero
	Low	Local / Collector	80 / 100	40 – 50	50 – 60	2	Low
Commercial	High	Collector / Sub-Arterial	100 / 150	20 – 30	30 – 40	3	High
	Low	Local / Collector	80 / 100	30 – 35	30 – 40	2	Limited
Office	High	Sub-Arterial / Arterial	200 / 150	10 – 25	20 – 35	2	High
Small Industry	High	Local / Collector / Sub-Arterial	80 / 100 / 300	10 – 20.	15 – 25	2	Low
Large Industry	High	Local / Collector / Sub-Arterial	80 / 100 / 300	15 – 20	20 – 30	3	High

Note: values represent topological characteristics of sampled networks (0.25 km^2) in the urban periphery of Lima. As a classification survey, only measures of the reference point or network were necessary.

an urban area with open spaces), urban growth boundaries (a line that separates urban and rural areas), and urban service boundaries (limiting the provision of public utilities) (Pramana 2016). Given that the Sleman Regency has partly become urban and partly rural, we consider it imperative to implement a fourth type of urban growth management strategy as a mid-range option between greenbelts and urban growth boundary lines. An agronomic urban boundary (AUB) network is proposed herein as large tracts of rural land, interconnected with point-specific development nodes, with assigned influence areas and mixed land-use economic corridors to form a revitalization network that promotes preservation and creation of new agricultural areas.

3.2. Methodology

First, travel routines were simulated to set the baseline results. Then, the OLUTM model was processed to evaluate future land use-transport interactions with output data seen in Fig. 2.

3.2.1. Transport component

A field survey was conducted in September 2019 in the affected areas of the Cangkringan sub-district. The data collected was processed and simulated with sociodemographic data in the transport component of the model to estimate travel utilities. Urban form measures were then incorporated to enable a comprehensive diagnosis of livelihoods in 2019.

3.2.2. OLUTM model (2019–2030)

The models in Fig. 3 reflect sequential steps for AUB network consolidation. It took seven data inputs from an exogenous data warehouse and ten sub-models sorted in two integration processes. The models are not expected to bring land use and travel to equilibrium because reality dictates that land use responds to the intensity of change. Therefore, the transport component evaluates travel performance on demand and the models are intended to reflect the observed behavior of agents. However, simplifications and abstractions of real behavior do exist.

4. Transport component

Data of this study including our data sample, a synthetic dataset, model instruments, and travel simulations are available in Mendeley Data ([Dataset 1] Garcia-Fry 2021).

4.1. Data

First, field observations and survey questionnaires were conducted in the Pagerjurang resettlement site to gather sociodemographic data and travel routines. Subsequently, online open municipal datasets ([Dataset 2] Indonesia 2020); ([Dataset 3] Indonesia 2018); ([Dataset 4] Indonesia 2018) and OpenStreetMap polygon data (OSM 2021) were sought for model input. Since high-quality spatial data is required, management with a Google Earth Engine (GEE) in a geographic information system (GIS) was essential for data integration processes.

The settlement was first partitioned into zones and HHs were randomly selected to represent a statistically accurate data sample. In-depth interviews took place with 41 Javanese citizens over three days, for 1–2 h each. The questionnaire (Supplementary Fig. S12-13), consisted of a census survey, activity-based schedules, Rolando Arellano's Lifestyle questionnaire (selected for its adaptability to

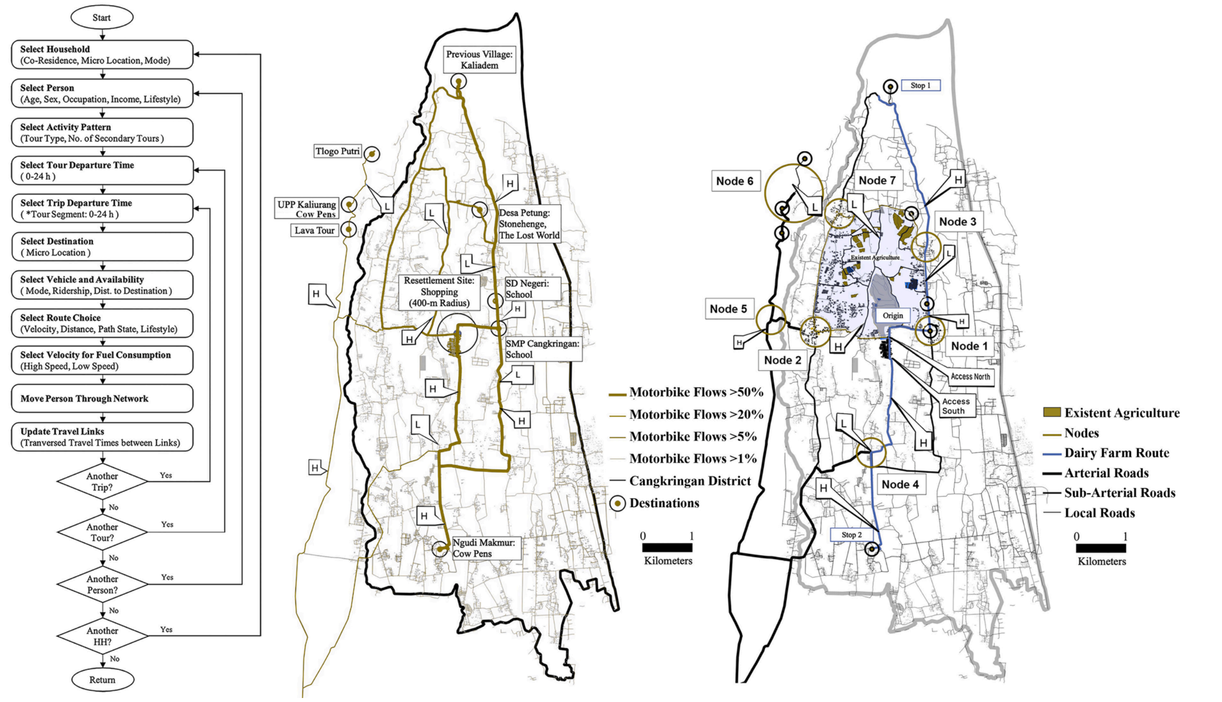

Fig. 4. The transport component (left). Travel flow classified with travel intensities, velocities, and road quality in the Cangkringan district (middle). The roads were structured with three types of hierarchies in edge-of-urban areas (right). (Color, 2 columns).

developing countries[1]), and HH location preferences with appropriate classifications for *peri*-urban areas (Lauf et al. 2012). The interviewed HHs accounted for 8.3% of the settlement and the refusal rate (the ratio of denied interviews over a total share), 10% of the settlement. Additionally, absent HH members contributed at a later date and all questionnaires were revised with a mapping activity to catalog travel schedules (Supplementary Fig. S11). Lastly, road networks were selectively sampled to extract the basic values of street attributes listed in Table 1. In accordance with Han et al. (2020), the appearance of cities may differ greatly, but the main pattern differences lie in intersection form and road density, as evidenced in (Supplementary Fig. S9).

4.2. Activity-Based schedules

Bowman and Ben-Akiva (2001) used the "primary destination" approach, assuming that one activity and destination are identifiable as a travel tour generator, representing a start and end time for the tour. We used this method to identify work destinations as the motivation for trip generation from Monday to Saturday, from 5:00 am to 4:00 pm (Mohammadi and Taylor 2019). The tour aggregation method, attributed to geographer Hagerstraand (1970), Chapin (1974), and Jones (1977) was used to retrieve a "home-work-other-home" schedule of activities reflecting daily travel routines. To model the individual activities of a population, a microscopic dataset is required. Therefore, we generated a synthetic population proportional to our data sample, where the 820 agents created have the same number of statistical features as the real population and only exist as files in the computer (more in Moeckel et al. 2003).

4.3. Travel simulation

To begin a travel microsimulation, first, identification of economic polar growth areas was reconciled with primary activities at the provincial level. Kaliurang, a small tourist town, and Yogyakarta represent two economic poles connected by a north and south axis road with "strategic" value (Pramana 2016). This road provides service through the Sleman Regency connecting the city to a growth destination (Sleman Regency, 2012). The local road network was surveyed to identify road hierarchies (local, collector, sub-arterial, and arterial), road widths (in width-meter lengths), and destinations structuring travel tours in Fig. 4. Travel schedules from our data sample, reflecting origins and stops made on the parcel (raster) level, were then used to identify locations using GIS. Sociodemographic data established travel route choices based on the shortest path with the least number of directional changes known to have a detectable impact in a study by Peponis et al. (2008). Sectoral speed identifiers, as either high (H) or low (L), were subsequently

[1] Publications are available only in Spanish. The English version translated by the authors is available in (Supplementary Fig. S13). Segment terms and definitions are available in (Garcia-Fry and Murao 2020).

Table 2
Travel tours in segments with distances, road widths, and route choices.

N.		Round Trip		Travel Route		Velocity Segments					Travel Distance (km)		
	Job Type	Travel Origins	Destination	Via	Mean Width (m)	1. High / R. Width	2. Low / R. Width	3. High / R. Width	4. Low / R. Width	5. High / R. Width	Low	High	Total
1	Farmer	Access North	Kaliadem	Jl. Kaliadem Raya	7.31	–	1,212 m / 7.75 *m*	1,286 m / 7.85 *m*	680 m / 7.29 *m*	3,053.7 m / 6.35 *m*	3.784	8.678	12.46
2	Farmer	Access South	Ngudi Makmur 1	Jl. Wukirsari	4.80	968 m / 3.62 *m*	1,438 m / 4.42 *m*	1,564 m / 7.10 *m*	693 m / 4.09 *m*	–	4.262	5.064	9.33
3	Tourism	Access North	Desa Petung	Jl. Petung Merapi	7.49	–	1,212 m / 7.75 *m*	702 m / 7.85 *m*	1,522 m / 6.88 *m*	–	5.468	1.404	6.87
4	Admin.	Access South	Hyatt Hotel	Jl. Kaliurang	–	–	–	–	–	–			17.90
5	Teacher	Access North	Negeri Cangkringan	Jl. Petung Merapi	7.51	–	1,212 m / 7.75 *m*	400 m / 7.28 *m*	–	–	2.424	0.800	3.22
6	Tourism	Access NW	Tlogo putri Jeep	Jl. Kaliurang	8.07	–	2,716 m / 6.87 *m*	3,057 m / 9.53 *m*	862 m / 7.82 *m*	–	7.156	6.114	13.27
7	Farmer	Access NW	UPP Kaliurang	Jl. Kaliurang	8.32	–	2,716 m / 6.87 *m*	2,672 m / 9.78 *m*	–	–	5.432	5.344	10.77
8	Tourism	Access NW	Stonehenge	Jl. Raya Merapi Golf	6.34	–	558.8 m / 6.36 *m*	1,950 m / 6.52 *m*	1,075 m / 6.15 *m*	–	3.268	3.900	7.17
9	Tourism	Access NW	Lava Tour	Jl. Kaliurang	8.35	–	2,716 m / 6.87 *m*	2,059 m / 9.83 *m*	–	–	5.432	4.118	9.55
10	Teacher	Access North	SMP Cangrinkgan	Unnamed road	8.00	–	950 m / 8.00 *m*	–	–	–	1.900		1.90

Note: Farming (66%), Tourism (24%), Administration (2.4%), Teachers (7.3%). The Hyatt Hotel is in the city.

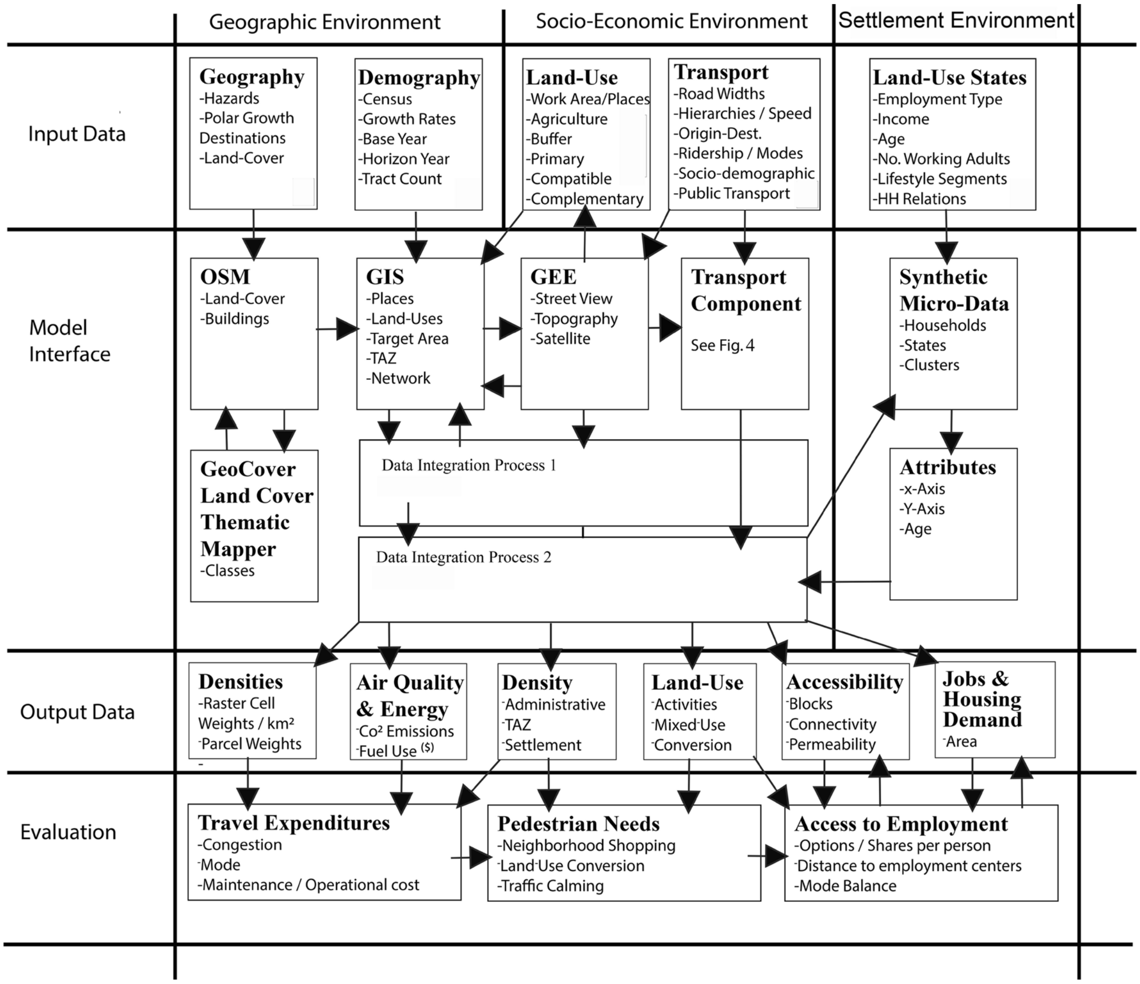

Fig. 5. Model integration flow. (B/W, 1.5 columns).

incorporated every 100–200 m, depending on roads (either paved or non-paved) and slope.

The consistent mode choice for single-occupant vehicles in Asia is the motorcycle, which was the only choice for farmers in Pagerjurang. The operation cost in suburban areas of Yogyakarta was calculated with fuel consumption in free-flow transit and potential traffic jams, with monthly maintenance and repairs of 3.00 USD and 11.00 USD, respectively (Herwangi et al. 2017). Here, 29.20 km/L of petrol in free-flow transit for Yogyakarta, with a speed of 42.42 km/h, represents a low performance *Lp* speed in the Cangkringan district (Sugiyanto 2016). While 45 km/L represents a high performance *Hp* speed, applied to a velocity of more than 55 km/h on straight, uninterrupted road segments. Fuel consumption is a function of tour distance *D*, factored by the sum of segments *i*, between an origin P_i and a destination P_j, under two mean performance levels.

$$F = \sum_{i=1}^{n} \left[\left(D_i \left(P_i - P_j \right) / Lp \right) + \left(D_i \left(P_i - P_j \right) / Hp \right) \right] P_l \tag{1}$$

Equation (1) estimates fuel consumption *F* subject to the local price per liter of fuel P_l for *n* number of road segments. Topography and weight were not considered due to a high probability (84%) of individual ridership for HHs with less than three adults, each possessing more than one vehicle. However, shared ridership was contemplated whenever a shared travel agenda was detected. The fuel price was set at 0.49 USD/L during the survey, and CO_2 emissions were estimated by multiplying the emission rate of a four-stroke motorcycle engine (55 g/km) by the total vehicle kilometers traveled (VKT) (Meszler 2007). Input data is shown in Table 2, defining access to the settlement as travel origins to calculate intra-settlement travel.

The following output data corresponds to the baseline results of this study. The daily fuel consumption totaled 5.22 USD and the mean estimation for monthly travel expenditures per person was 20.39 USD, equal to 26% of the average monthly income (78.15 USD). We also registered 22,519 g of CO_2 emissions from the 421 VKT daily with 8% (33.56 km) originating inside the settlement. Farmers, tourist vendors, administrators, and teachers travel 35%, 40%, 19%, and 6% of the total distance, respectively. They spend in average 3.91 USD more than people in other disadvantaged areas of Yogyakarta DIY (see Herwangi et al. 2017, p.6). These results revealed a

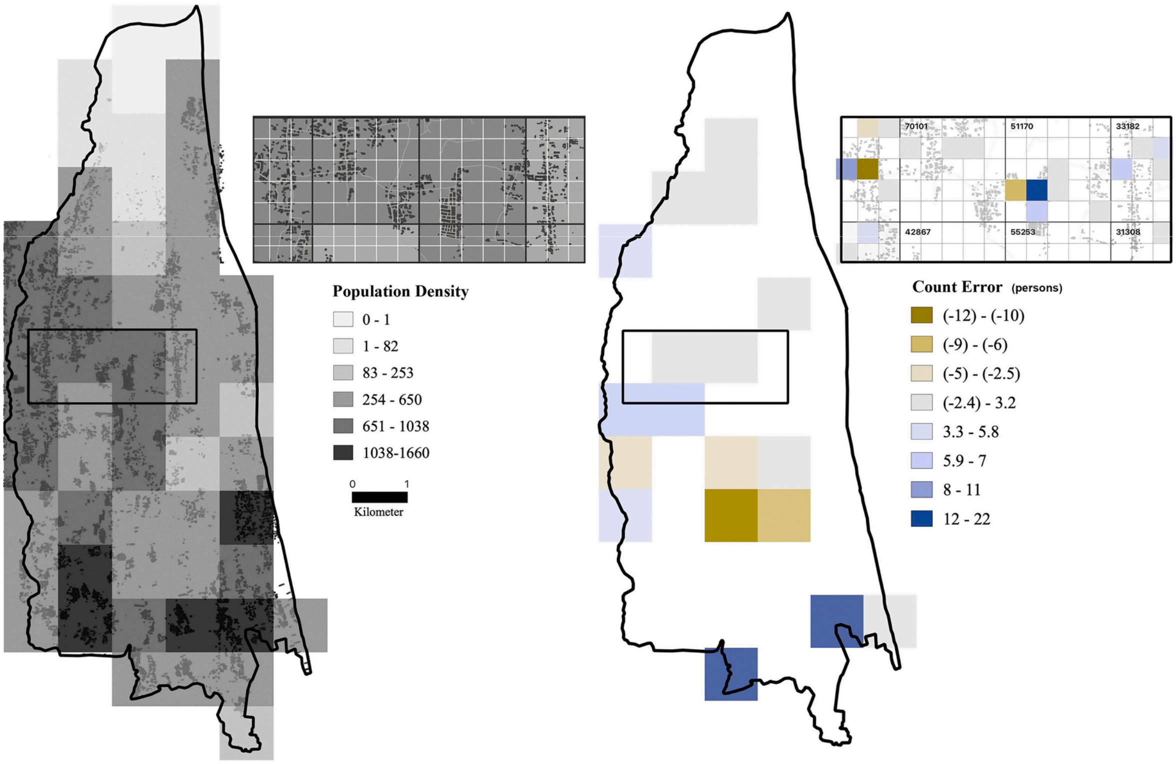

Fig. 6. Density map of the Cangkringan district in 2019. The inset box defines the TAZ's boundary with ancillary data in a 200-meter spatial resolution and the Pagerjurang resettlement site located in the 51,170 (m^2) "parent" raster cell. A map of the count error by block for the dasymetric map to the right is shown with class intervals by standard deviation from the mean error, which is zero. Green areas indicate underestimation while blue areas indicate overestimation. (Color, 2 columns). (For interpretation of the references to color in this figure legend, the reader is referred to the web version of this article.)

restrained potential to increase HH profits after utilizing 26% of the average monthly income for travel. This is exacerbated by the low-income margins and the limited access to livelihood options for middle-aged people and the elderly.

5. OLUTM model (2019–2030)

The model system in Fig. 5 divides compact modules into three environments: The geographic environment, the socioeconomic environment, and the settlement environment.

5.1. Geographic environment

5.1.1. Territorial analysis

The first module uses future population projections estimated with conglomerate statistical trends (fertility, birth, mortality, migration, etc.), subject to past and current data, and assumed to continue. The local government's statistical census bureau (Statistik Badan Pusat Kabupaten Sleman) offers open datasets for the district's population and its growth rate from 2010 to 2017 ([Dataset 3] Indonesia 2018). The projections for 2019 and 2030 using the district's growth rate (0.5%) resulted in 29,740 and 31,302 people with densities of 619 and 652 people/km^2, respectively (Supplementary Eq. S1 and S2). These values were validated after comparing the 2018 population count with the government-recorded count in ([Dataset 4] Indonesia 2019).

5.1.2. Density redistribution

The Cangkringan sub-district has a 48 km^2 area and is expected to have an increase of 33 people/km^2 by 2030. Open source 2019 building footprint polygon data (OSM 2021) were compiled and used as ancillary data for a dasymetric redistribution of the census-based district population count. We used this method to distribute a total count (population census) across an area (administrative/census unit). Instead of distributing the count equally by areas, land cover data were used at a finer spatial resolution to unequally distribute the total count in weights reflecting a more accurate distribution of people over the study area.

Selective sampling of the ancillary data in a km^2 raster cell grid was compiled and GeoCover Landsat Thematic Mapper (TM) classifications from MDA Federal Inc. (1995–1997) were normalized to accurately classify the samples in our target district. The first redistribution of density weights was possible using these samples. Subsequently, a 4.17 km^2 TAZ was traced around the Pagerjurang

Table 3
Road network types.

<table>
<tr><th rowspan="2">Width (m)</th><th rowspan="2">Road Type</th><th colspan="3">Type 1</th><th colspan="4">Type 2</th><th colspan="5">Type 3</th></tr>
<tr><th colspan="3">Local
r =300 (m)
(H:W)</th><th colspan="4">District
r =600 (m)
(H:W)</th><th colspan="5">Inter-District
r =900 (m)
(H:W)</th></tr>
<tr><td>3 – 4</td><td>Local Road</td><td rowspan="2">1 : 1.5</td><td></td><td></td><td></td><td></td><td></td><td></td><td></td><td></td><td></td><td></td><td></td></tr>
<tr><td>4 – 6</td><td>Local Road</td><td rowspan="2">1 : 1.5</td><td></td><td></td><td></td><td></td><td rowspan="4">1 : 2</td><td></td><td></td><td></td><td></td><td></td></tr>
<tr><td>6 – 8</td><td>Collector Road</td><td></td><td rowspan="2">1 : 2</td><td rowspan="2">1 : 1.5</td><td></td><td></td><td></td><td></td><td></td><td></td><td></td></tr>
<tr><td>8 – 10</td><td>Collector Road</td><td></td><td></td><td rowspan="2">1 : 2</td><td></td><td></td><td></td><td></td><td></td><td></td></tr>
<tr><td>15 - 18</td><td>Arterial Road</td><td></td><td></td><td></td><td></td><td rowspan="2">2 : 1</td><td rowspan="2">2 : 1</td><td></td><td></td><td></td><td></td></tr>
<tr><td>18 - 21</td><td>Arterial Road</td><td></td><td></td><td></td><td></td><td></td><td></td><td rowspan="2">2 : 1.5</td><td></td><td></td><td rowspan="4">3 : 1</td></tr>
<tr><td>24 - 30</td><td>Expressway Road</td><td></td><td></td><td></td><td></td><td></td><td></td><td></td><td rowspan="2">2 : 1</td><td></td></tr>
<tr><td>28 - 30</td><td>Expressway Road</td><td></td><td></td><td></td><td></td><td></td><td></td><td></td><td></td><td rowspan="2">0.5 : 1</td></tr>
<tr><td>16 - 32</td><td>Highway Road</td><td></td><td></td><td></td><td></td><td></td><td></td><td></td><td></td><td></td></tr>
</table>

Note: Areas of the Sleman Regency were sampled to measure road widths, network hierarchies, and enclosure ratios. Roads are classified with 4 types found to establish commonalities among sampled networks (Han et al. 2020). Highways were also sampled to fit the model. Enclosure ratios follow a height-to-width ratio rationale of 3/4 for urbanized areas (Alkhresheh 2007, p.139) and 17/20 as the local equivalent for nodes of the TAZ.

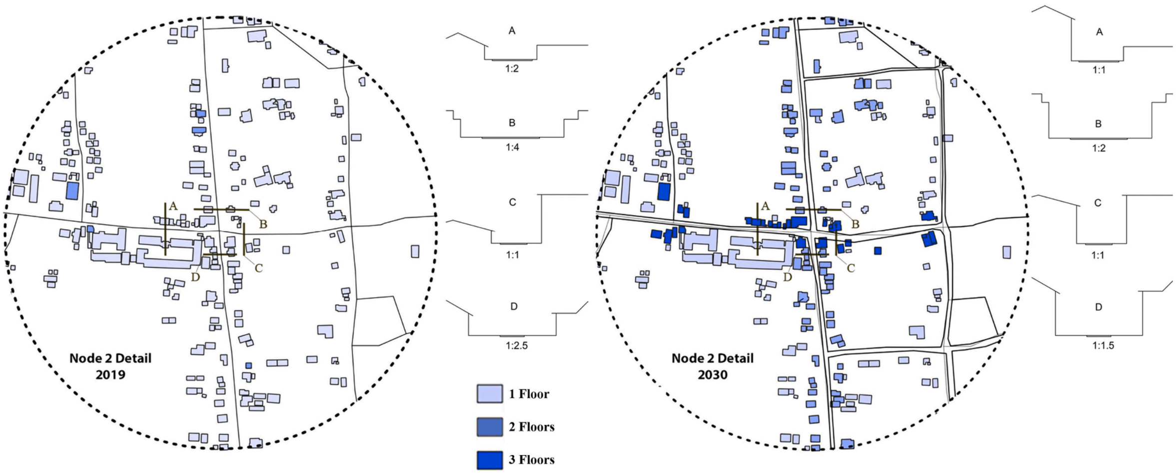

Fig. 7. Built capacity of buildings sharing a side with intersecting roads. (Color, 2 columns).

resettlement site shown in Fig. 6. We used building footprint areas from a 200 m spatial resolution raster grid and interpolated them with each km^2 "parent" raster cell's density weight to redistribute densities to a higher resolution. Land cover normalization was carried out following the methods of Mennis and Hultgren (2006), Gaughan et al. (2013), Stevens et al. (2015), and Linard et al. (2011). The projected population count in the TAZ was 3,409 (2019) and 3,590 (2030) with a total of 181 new persons by 2030 and a 92.4% accuracy with deviation range of $\pm$ 17 persons (Supplementary Table S3). Ages below 18 (29%) ([Dataset 2] Indonesia 2020) were then excluded from the count, leaving 128.5 adults.

5.1.3. Node weight estimation

The projected population reflects young adults with higher education living in the target area and having similar profiles, values, and attributes of those surveyed in 2019 (compatible with testimonies in Miller M.A., 2018, p.202). Residential preferences for social neighborhoods (71%), areas surrounded with amenities (12%), and in central areas (10%) were used to estimate the number of adults choosing to live in serviced areas (119.5 adults). Subsequently, nodes identified in Section 4.3 were assigned a typology from Table 3 by evaluating road volume capacity at the junction level (in width-meters length). Each road adopted a street enclosure ratio (height: width) to set a built capacity and an influence radius (r) to limit that growth. Enclosure ratios were estimated with theoretical constructs found in Alkhresheh (2007) and Rudlin and Falk (1999) to target urban environments with rural streetscapes. The model aggregated road volume capacities per node and used those weights to distribute adults among nodes with the same scale: 61 in node 1 and 58.5 in node 2 (Supplementary Fig. S4).

5.1.4. Housing demand

This module estimated the demand for new adults using HH compositions sourced from our data sample to retrieve the percentage of adults per household (APH): 1-adult (52%), 2-adults (32%), and 3-adults (or more) (16%). These ratios were then applied to the 61 adults in node 1, totaling 45 HHs partitioned into 32 (1-adult), 10 (2-adult), and 3 (3-adult) HHs, followed by node 2 with 43 HHs, partitioned into 31 (1-adult), 9 (2-adult), and 3 (3-adult) HHs.

Table 4
Local multipliers for tradable, non-tradable, and agriculture jobs in the Cangkringan district.

	Tradable (T_1)			Non-Tradable (NT)			Agriculture (A)		
	OLS	IV	Additional jobs for each new job	OLS	IV	Additional jobs for each new job	OLS	IV	Additional jobs for each new job
	1	2	3	4	5	6	7	8	9
T				0.703** (0.45) [0.08]	1.207*** (0.249) [0.644]	2.95 (0.021)	−1.26** (0.81) [1.419]	−2.88*** (0.508) [0.713]	−2.09 (0.002)
NT	0.113** (0.072) [0.08]	0.533*** (0.11) [0.64]	1.51 (9.78E-5)				−1.05* (0.277) [0.341]	−2.14*** (0.211) [0.887]	−0.58 (0.000)
A	−0.062*** (0.040) [0.08]	−0.246*** (0.043) [0.712]	0.68 (0.000)	−0.322*** (0.084) [0.341]	−0.414*** (0.0409) [0.887]	0.37 (0.278)			
T_2	0.379*** (0.124) [0.25]	1.01*** (0.015) [0.996]	1.96 (0.005)						

Note: The estimation results are depicted for combinations between tradable, non-tradable, and agriculture employment change. The table includes both the ols and the instrumental variable estimation. Standard errors are in parenthesis and r-square values in brackets. P-values are significant at ***99%, **95%, *90%.

The model proceeded using residential surface areas from resettlement studies in Sleman and an HBE study in Malang to estimate spatial requirements. In Sleman, HHs received 36 m^2 houses on 100 m^2 lots. However, most of them expanded their housing coverage to the maximum footprint available (Maly et al. 2015). Also, lot sizes were deemed insufficient for large families (Singghi and Asano 2019, p.120). Therefore, we assigned lots of 70 m^2 (1-adult HH), 100 m^2 (2-adult HH), and 120 m^2 (3-adult HH) considering the size of families with HBEs (Tutuko 2014, pp.51–63), thus resulting in 3,600 m^2 (node 1) and 3,430 m^2 (node 2) coverages.

Using a Google Street View built-in environment, we recorded the current (2019) building heights in node influence areas and estimated the potential building capacity of each node with the assigned enclosure ratios as in Fig. 7. A user-based input was required to establish the mean inter-story height from our survey (Supplementary Table S4). Then, the model queued lots in asphalted roads having 25.4% higher value according to Pramana (2016) and estimated the built capacity of nodes 1 (20,555 m^2) and 2 (10,589 m^2).

5.2. *Socioeconomic environment*

5.2.1. *Land-Use designations*

In this module, primary activities were classified and new activities were assigned as user-based inputs to trigger local employment in the TAZ. First, land uses were surveyed with Google Street View to classify nodes with a land-use category (residential, commercial, light industry, or service). A category was assigned by identifying primary activities factored with intersection proximity. Primary activities maximize business utilities attracting people from various scales of a city, depending on the degree of specialization.

We classified node 1 as "local-institutional; service" and node 2 as "local-educational; service" (node type-primary activity; land use). Both were identified as service nodes because the primary activity belongs to this land use and attracts people from the local district. We then assigned a technical research institute compatible with node 1 (4,060 m^2), a cultural language institute (4,027 m^2), and a medical veterinary center in node 2 (2,300 m^2). The model distributed them unevenly to reinforce the node with less potential for development. A total of 164 job positions were estimated with density ratios (floor-space requirement per employee), built corridors (10%), and a 20% gross external to net internal space transition (Dancer 2015).

5.2.2. *Employment distribution*

This module simulates the multiplier effect, classified into sectors based on the Ministry of Manpower and Transmigration which separates labor within the local economic structure. Employment values were sourced from the Secretariat Governance Bureau of Population for Yogyakarta DIY (a translated version is available in [Dataset 1] Garcia-Fry 2021).

The model factors local multipliers to capture the demand for local services following an empirical study by Moretti (2010), to estimate long-term employment of a local area as a result of attraction to a successful firm or service. There is a shock in employment for tradable jobs under agglomeration effects and for non-tradable sectors. Tradable jobs follow a logic of domestic manufacturing with production consumed in a different geographic entity. Informality was also considered, contributing to the size of multipliers related to informal jobs often created in developing countries (Charpe 2019). The model proceeds as follows:

$$\Delta N_{c,t}^{NT} = \beta \Delta N_{c,t}^{T} + \eta X_{m,t-1} + \varepsilon_{c,t} \tag{2}$$

Equation (2) captures the relation between the change in the tradable sector, $\Delta N_{c,t}^{T}$, and the change in the non-tradable sector, $\Delta N_{c,t}^{NT}$, measured in an administrative entity c with an error term $\varepsilon_{c,t}$, and regressor coefficients β and β'. Population size of the last term is denoted by $X_{m,t-1}$ with an elasticity coefficient η. We used six observances for all entities in the sub-district's census (2015–2020) to

Table 5
Sensitivity of job location choice variables.

	Regression Scores	Maximized Model				
Variables	***Coefficients***	***Coefficients***	***Min***	***Max***	***Probability***	***Likelihood Ratio Test***
Intercept	1.364*** (0.226)	1.895*** (0.210)	1.34	2.45	2.30	−13.51
Vacancy	−0.032* (0.024)	−0.042*** (0.022)	−0.10	0.02	1.00	−11.84
Built Density Ratio	0.994*** (0.202)	0.838*** (0.187)	0.34	1.33	1.26	−12.30
Building Capacity	0.002 (0.002)	0.003*** (0.002)	0.00	0.01	1.00	−11.84
Land Value	−0.057** (0.021)	−0.051*** (0.020)	−0.10	0.00	1.00	−11.85

Note: ***significant at 99%, **significant at 95%, *significant at 90%. Standard errors are in parenthesis. Building capacity did not have significant effect on location choice. Land value accounts for job density ratios making them significant predictors. The regression and a Lorenz-curve distribution for location choice is reported in (Supplementary Fig. S5). F-test is significant at 99% with 7.78. Chi-square = 4. Predictive efficiency = 91%.

estimate local multipliers.

$$\Delta N_{c,t}^{T1} = \beta' \Delta N_{c,t}^{T2} + \eta X_{m,t-1} + \varepsilon_{c,t} \tag{3}$$

Equation (3) was used to find the changes in the tradable sector $\Delta N_{c,t}^{T1}$ for sub-sector *T1*, having a shock effect on the rest of the tradable sector $\Delta N_{c,t}^{T2}$, in administrative entity *c*. Equations were computed with a standard ordinary least square estimation. This method has two limitations: (1) reverse causality and (2) omitted variable. An instrumental variable estimation followed to verify the results based on the shift-share approach coined by Bartik (1991) for tradable, non-tradable, and agricultural sectors. The instrument assumes that a change in national employment is unrelated to the local labor market. However, the net change of administrative entity *c* replaced the national employment in $t - s$ as a weight for variance.

$$\Delta N_{m,t}^{T} = \sum_{j \in T} N_{j,c,t-s} \left(\log\left(N_{j,t} - N_{j,c,t}\right) - \log\left(N_{j,c,t-1} - N_{j,c,t-s}\right) \right) \tag{4}$$

Equation (4) estimates the inner product change of industry-location shares for tradable employment $\Delta N_{m,t}^{T}$ and the local industry growth rate by subtracting the log change in national employment $(N_{j,c,t-1} - N_{j,c,t-s})$ from the log variance in local sectoral shares $(N_{j,t} - N_{j,c,t})$. Multipliers for the Cangkringan sub-district can be seen in Table 4, with 2.95 non-tradable jobs for each tradable job added, and 2.09 agricultural jobs removed. One tradable sub-sector job created 1.96 jobs in the tradable sector, confirming the existence of agglomeration economies.

Multiplicity values were applied to the pool of jobs in 2020, adding 840 jobs (2020–2025) and 1,417 jobs (2025–2030). For job removals, the vacancy relative to that space became available to other jobs in that sector. Removals added to 88 tradable jobs secured by HHs with higher education (from sub-section 5.1.3), and 36 entrepreneurship jobs for commercial vendors of Pagerjurang. Negative coefficients deducted 183 agricultural jobs and 6 entrepreneur jobs confirming the trend in rural labor and totaling 1,944 new jobs (Supplementary Table S6).

5.2.3. *Employment allocation*

The model for job allocation applies variables that follow traditional bid-rent literature in urban economics. Access to people is expected to increase bids on commerce and service venues closer to intersections where the density is higher. In this module, we allocated jobs with a multinomial logit model to estimate the probability of a company choosing a location among the alternative vacancy areas in proportion to the built capacity of a node.

Jobs were located in non-residential lots using floor-space density ratios (square-meters per employee) with the entrepreneur sub-sector in residential lots sharing a side with roads. Vacancy in node 1 totaled 20,555 m^2 with 1,200 job vacancies, 5,687 m^2 of residential area, and 5,224 m^2 of residential space subject to land-use conversion. In node 2, a total of 18,255 m^2 were recorded, with 830 job vacancies, 7,817 m^2 of residential area, and 2,379 m^2 of residential space subject to conversion. Vacant lots in node 2 (26.5% of the recorded total) were included in the pool of HH vacancies for families that migrate in search of employment.

First, the allocation choice model used variables found by Pramana (2016) to explain land pricing with the shortest path to services and with job density ratios to determine a land value coefficient. A Monte Carlo sampling process followed to generate a decision as to whether a job would be placed, subject to the accommodation of that job. Sectors were ranked to compete for vacancies using a discrete random sampling distribution constrained by the log-likelihood coefficient of the job's density ratio. A final decision was based on whether the mean log-likelihood and standard deviation of the real estate coefficients in Table 5 were higher than 1. This followed a variant of the location choice model in the Urban Sim with the logic that all jobs *j* from a given sector *s* are paired to a location *l* with a probability *p*:

$$P_s = \left\{ (j,l) | j \in J_s, l_s \in L_s^J, \text{sectoralsetofjobpairsandlocations} \right\} \tag{5}$$

$$T_s = \left\{ j | j \in J_s, \forall l \in L_s^j (j,l) \notin P_s \right\} \tag{6}$$

$$J_s = \left\{ l | l \in L_s^j, \forall j \in J_s (j,l) \notin P_s \right\} \tag{7}$$

Table 6
Sensitivity of HH location choice variables.

	Regression Scores	*Maximized Model*				
Variables	***Coefficients***	***Coefficients***	***Min***	***Max***	***Probability***	***Likelihood Ratio Test***
Intercept	0.903*** (0.269)	0.707*** (0.175)	0.24	1.17	0.71	−24.85
Vacancy	−2.500** (1.177)	−1.287* (0.77)	−3.32	0.74	0.08	−20.37
Built Density	1.413*** (0.241)	0.788*** (0.157)	0.37	1.20	0.80	−22.27
Building Capacity	0.026** (0.012)	0.013* (0.007)	−0.01	0.03	0.51	−24.17
Land Value	−0.859** (0.363)	−1.021*** (0.237)	−1.65	−0.40	0.30	−23.10

Note: ***significant at 99%, **significant at 95%, *significant at 90%. Standard errors are in parenthesis. Built density is a good location choice predictor with land value negatively correlated, hence the preference for lower prices in nodal areas. The regression with a Lorenz-curve distribution for location choices is available in (Supplementary Fig. S6). F-test is significant at 99% with 23.23. Chi-square = 4. Predictive efficiency = 81%.

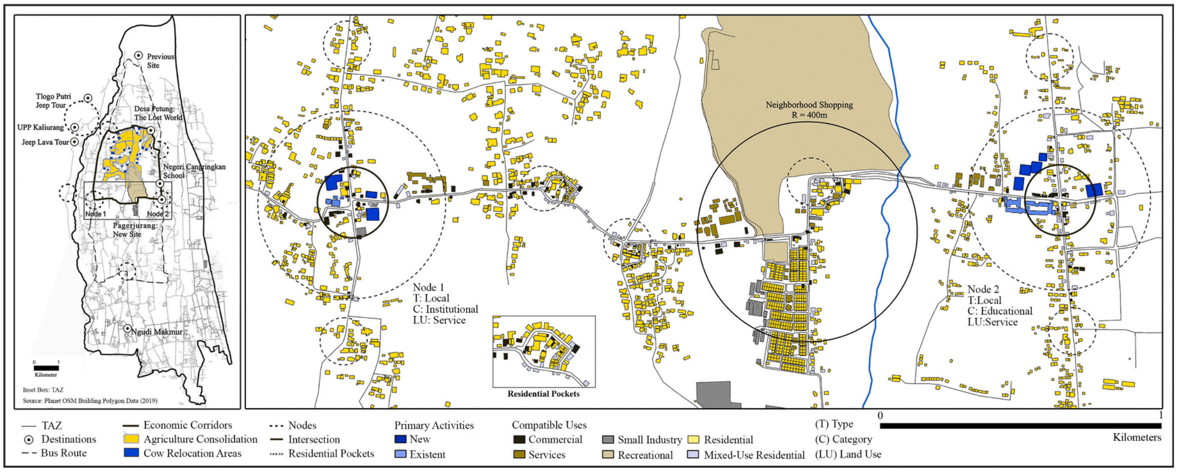

Fig. 8. Land uses by 2030. New primary activities caused mixed-use development between the nodes. The inset box shows the AUB network with consolidated agricultural areas and cow relocation sites. The aggregation of dairy farming inside the network would contribute to further reduce VKT. A tentative public bus route is established to simulate its feasibility and promote directive extensions of the network. (Color, 2 columns).

$$F_s = \{(l, p) | l \in J_s, d\text{enotingtheprobability}p\text{ofajob}j\text{locatingin}l\} \tag{8}$$

Equations (5) to (8) trial sectoral jobs competing for geo-coded sectoral vacancies with land value coefficients. Once allocated pairs were removed, the 160 non-tradable jobs left were assumed to hold vacant residential lots in node 2, totaling 9,523 m^2 of HBEs. The housing demand then surged (137,520 m^2) with a comparatively low offer (26,016 m^2), causing nodal spillovers.

5.2.4. Spillover management

In-migration was addressed with a land-use treatment on “edges” of the network (i.e., the connection between nodes) (Nystuen and Dacey 2005; Arlinghaus et al. 2002). This follows regional accessibility, urban economics, and social urban theory with the general assumption that HHs place a higher bid on parcels with access to services, bus stops, and markets (Rhondi et al. 2018; Alonso 2013). This is common for people seeking employment in urban agglomerations where changes in land price account for vacancy rates and intensity of use.

This module used a multinomial logit model to find the probability of location choices for census-based and in-migrating HHs. As in the employment allocation model, they were sectored and ranked with a discrete random sampling distribution using income ratios from our data sample. This was done to pair competing HHs with vacancies in nodes using the Monte Carlo instrument. Constraints included vacancies below 70 m^2, 100 m^2, or 120 m^2. A final decision was based on the mean and standard deviation of the log-likelihood for variables listed in Table 6. A total of 301 pairs were allocated and removed from the pool of HHs and locations.

To accommodate the overspill, the edge was assigned with an enclosure ratio from Table 3 expanding the pool of vacancies by 5,658 m^2. The resettlement site boundary road also delivered 2,620 m^2. The model then used a value for non-working adults (16%) in the sub-district ([Dataset 2] Indonesia 2020) to provide an estimate for housing demand in node 1 (75,079 m^2) and node 2 (36,425 m^2). These were divided by the number of intersecting roads in each node to distribute that demand along segments of an edge and consolidate the network.

The model proceeded to pair 75 HHs with new vacancies, leaving a deficit of 19,598 m^2. Residential demand weights ***RDW*** were then used to supply that deficit in a vector of ***n*** terms with segments ***W*** of 400–800 m each from the midpoint of the edge to each node;

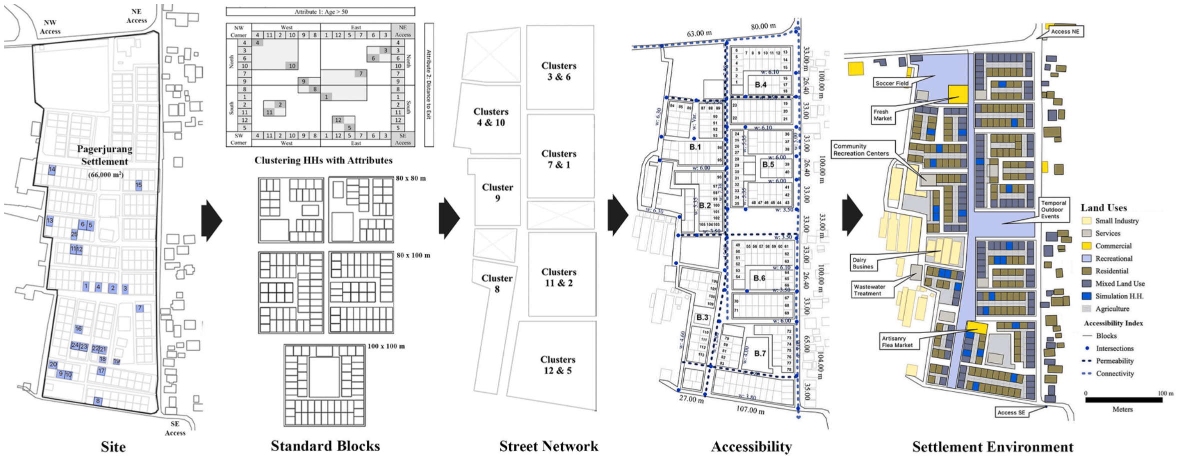

Fig. 9. Settlement simulation process. A total of 113 mixed-use vacancies became available for HBEs. Note that road hierarchies are a product of sampled networks in Tables 1 and 3. (Color, 2 columns).

Table 7
Predictive capacity of the model.

	Regression Scores			Maximized Model			
Variables	**Coefficients**	**Min**	**Max**	**Coefficients**	**Probability**	**Log-Likelihood**	**Likelihood Ratio Test**
Intercept	0.227 (0.161)	−0.19	0.65	0.465			
Risk-Taking Levels	0.484*** (0.042)	0.37	0.59	33.682	1.00	−1.75	−6.75
Occupation Classes	0.226*** (0.070)	0.04	0.41	1.585	0.83	−0.37	−5.37
Education	0.075*** (0.024)	0.01	0.14	−0.380	0.41	−0.37	−5.37
HH Composition	−0.291*** (0.045)	−0.41	−0.17	−13.602	0.00	−0.37	−5.37
Income	0.010*** (0.002)	0.01	0.01	0.414	0.60	−0.37	−5.37
Mean				3.69	0.57	−0.65	−5.65
Standard Deviation				15.75	0.39	0.62	0.62

All P-values are significant predictors excluding the y-intercept. Standard errors are in parenthesis. Farming was constrained as a median value to train our data. Results indicate that HH composition (with negative correlation to land-use change) does not predict ventures. However, income and risk-taking segments have the largest predictive outcome. This is because size is not the only factor to affect business ventures. In reality, education may seem more appropriate to measure livelihood diversification, but it does not stimulate changes in the region yet. It is, however, well understood that education is a major driver of specialization, but does not necessarily imply occupational multiplicity.

$$\boldsymbol{RDW} = \boldsymbol{a}\boldsymbol{W}_1 + \sum_{i=1}^{n} \boldsymbol{a}(\boldsymbol{W}_i - \boldsymbol{i}) \tag{9}$$

Equation (9) distributes the remaining demand to segment weights with vacant lots added as user input to the data warehouse. Lots were classified as bare areas and developed as residential pockets with mixed uses shown in Fig. 8. By our definition, these are HHs around a public space with access to the road network. The allotment left a 12,202 m^2 (44%) housing deficit.

5.3. Settlement environment

5.3.1. Street network

Development of the edge was expected to have a substantial effect on livelihood diversification. Therefore, a clustering model grouped displaced HHs with travel attributes to locate them in a simulated settlement and evaluate micro land-use change. First, the model clustered part of our synthetic dataset into 12 neighborhoods of 26 HHs each. Note that this number considers the average of the neighborhood system in Indonesia (20–40 HHs) and the average of manageable decision-making neighborhoods (20–25 HHs) according to McCamant et al. (1994). Destinations and demographic data were used to weigh the polarity of travel attributes on-site. A majority of farmers travel to a dairy cooperative south of Pagerjurang. Therefore, the variables selected were: south destinations for the y-axis and age-above-50 for the x-axis. The latter established a control variable for the labor force currently affected by travel, testing our hypothesis that under equal access to customers, HBEs are driven by income, HH composition, and risk (changing residential land-use structures to mixed-use development).

The settlement module followed to locate HH clusters in a road network. A residential category was selected from Table 1 to define the permeability level. Then, blocks of 80 m and 100 m lengths were populated with 120 m^2 lots to accommodate HHs of all sizes. User inputs included recreational areas (2.5 m^2/person), agricultural areas (35 m^2/lot), and religious buildings as constituents of the local

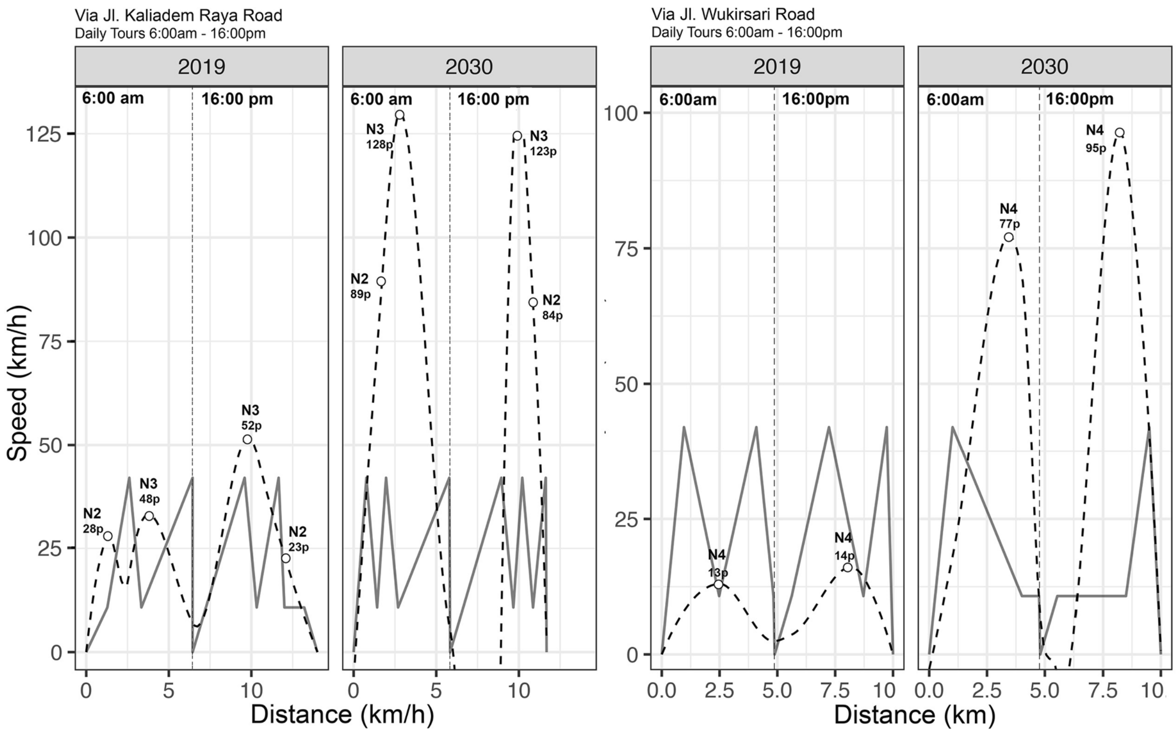

Fig. 10. Vehicular congestion at peak hour transit (nodes 2,3 and 4). The curve shows congestion levels, while lines follow velocity change in the dairy farming route (Fig. 4). Most trips are made through Kaliadem Raya road to farmlands. Then, they travel south through Pagerjurang to Wukirsari, where dairy cooperatives were relocated totaling 21.8 km round trips. Congestion was estimated for 15-minute intervals. (Gray, 1.5 columns).

culture. Then, each block was sub-divided into 26 m, 33 m, or 65 m lengths to stimulate walking in slow travel environments (Krizek 2003). Given that landmarks were found to influence navigational decisions by Millonig and Schechtner (2007), a market and a large open space were included to guide potential customers through the road network. Then, road widths were selected from Table 3 to model the settlement in Fig. 9.

5.3.2. Land-Use change

This last module evaluates the relationship between accessibility and sociodemographic data to explain land-use change. Access to people, income, and HH compositions are considered to facilitate economic activity (Tutuko 2014). Also, livelihood diversification associated to services in the region is related to the percentage of motorcycle ownership (70%) (Rijanta 2009). Therefore, this model focused on HBEs with farming as the primary occupation.

A logit model was used to identify the intensity of demographic effects on land-use change with our data sample (e.g., see Sun and Robinson 2018). We assumed that livelihoods diversified by 2019 reflect a choice of land-use change, subject to the increment of people (Rijanta 2008). A regression followed to evaluate farming with a nominal value between commerce and services and compare the efficiency of variables in (Supplementary Table S8).

Using the HH allocation model, agents were extracted from our synthetic data to pair HHs with mixed-use vacancies relative to their block. Land-use change was constrained by the mean income of segmentations found to take higher risks in (Garcia-Fry and Murao 2020). These thresholds were used to train our data and maximize the model's predictive accuracy shown in Table 7. The outcome revealed that 94 HBEs (84% of the lots) diversified their livelihoods with 61 farmers in 59 HBEs (63% of HBEs) complementing rural labor.

5.4. Transport component

A random selection of 25 HHs and 41 agents was performed to initiate the transport component. Intra-settlement travel was simulated to evaluate allocation with travel attributes. Routines were then established and simulated to account for travel utilities. Diversified HHs were not considered for scheduling adjustment because their primary occupations were unchanged.

5.4.1. Travel within the settlement

To begin the simulation, all origins and destinations were reconfigured. The shortest paths to destinations were measured, enabling agents with destinations within a 400 m radius from their lot to presumably walk. Pedestrians sell their farm produce in the

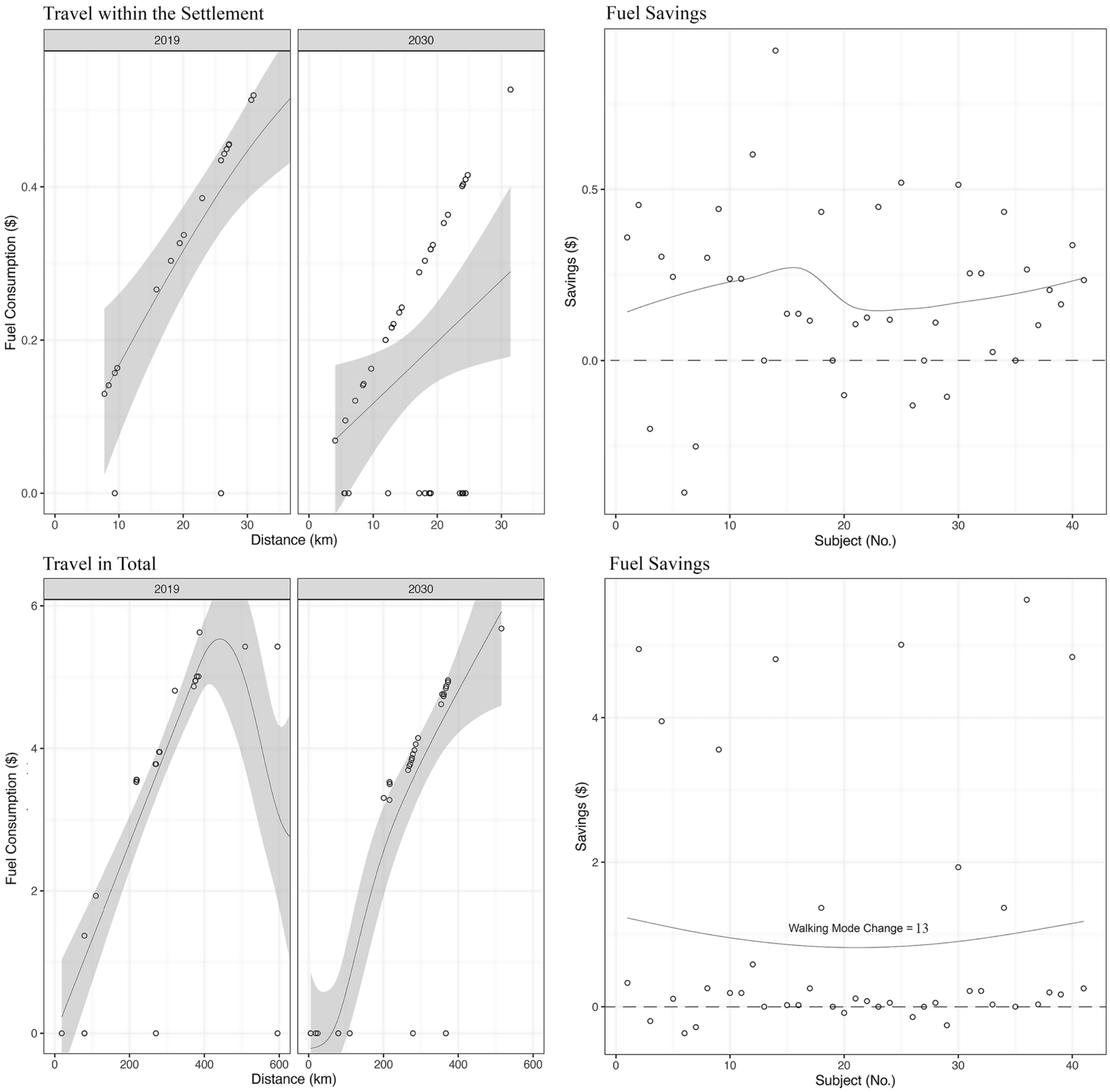

Fig. 11. Comparative assessment of fuel consumption. Smoothed trend lines use Gaussian regression with a confidence interval affected by multi-modal travel, thus resulting in utility savings (right). Density conveys to low amount of savings when correlated with congestion and compared to modal shift, causing the majority of travel savings. The latter provides an indication of shorter intra-tour distances. (Gray, 1.5 columns).

settlement's market or work in the nodes nearby. Consequently, the vehicle occupancy rate decreased by 50% (compared to the base year). This simulation was performed with motorcycles moving at low speeds.

Intra-settlement travel denotes a 55% reduction of cumulative travel distance. This indicates that HH allocation with individual attributes had a substantial effect on travel efficiency. Consequently, 49% less fuel consumption was observed–88.73 USD savings for the entire settlement. Additionally, walking modes detracted 45% energy consumption and CO_2 emissions as a result of nine agents (22%) living closer to their workplaces.

5.4.2. *Travel in total*

New travel agendas were processed for those who secured a non-tradable job in nodes 1 and 2. Walking shares increased to 13 persons (32%) and congestion in nodal areas decreased travel speed adding expense to each tour as shown in Fig. 10.

Travel through congested areas increased fuel consumption, but nearby workplace areas conveyed higher rates of modal shift. The effect was reflected in 20% less vehicle ownership for agents with new jobs near their lot. VKT were reduced by 23%, consequently dropping fuel consumption by 28%, thus improving on travel performance as depicted in Fig. 11.

Table 8
Monthly travel expenditures.

			2019		2030		Total
		Agents	**Dist. (km)**	**Fuel (USD)**	**Dist. (km)**	**Fuel (USD)**	**Savings (USD)**
1	Travel in Settlement	41	1007.01	14.97	452.80	7.60	7.37
			100%	100%	45%	51%	49%
2	Travel in Total	41	12,632	156.5	9,687	112.2	44.32
			100%	100%	77%	72%	28%
3	Travel Utilities	41		836		590	246
				100%		70%	30%
4	Expenditure per Person (income %)	1		20.39 (26%)		14.38 (18%)	6.01 (30%)
5	Expenditure per Household	1		33.43		23.58	9.85
6	Before Intervention (2019) (2030)	528 / 605		10,766		12,336	3,636
7	After Intervention (2019) (2030)	528 / 605		7,598		8,700	
8	Savings after Implementation	528 / 605		3,168		3,636	

Note: All values are in USD and pertain to 41 travel diaries sought in the Pagerjurang settlement. Hypothetical statements exemplify the results to illustrate the temporal effects of implementation after resettlement in 2010.

Table 9
Model assumptions.

Section	**Module**	**Description**	**Theoretical Logic**	**Reference**
5.1.1	Territorial Analysis	The government-recorded population growth rate is assumed to continue (the change in population over unit time period).	Population Growth Rates Cohort models	Statistical Census Bureau
5.2.2	Employment Distribution	The shift-share approach assumes that a change in national employment is unrelated to change in the local labor market.	Shift-Share Approach (National employment change replaced with district variance)	Charpe 2019
5.2.3	Employment Allocation	160 Non-tradable jobs were assumed to take hold of vacant lots in node 2, thus becoming HBEs.	Bid-Rent Theory of urban accessibility.	Alonso 2013
5.2.4	Spillover Management	Relocating HHs place higher bids on lots with access to serviced areas.	Accessibility, Urban Economics, and Social Urban Theory.	Rhondi et al. 2018; Alonso 2013
5.3.1	Street Network	HBEs are driven by income, HH composition, and risk.	Prospect Theory	Kahneman and Tversky 1979
5.3.2	Land-Use Change	Livelihoods currently diversified reflect a choice of land-use change subject to a rise in people.	Relative Location in Bid-Rent Theory.	Rijanta 2008

6. Discussion and concluding remarks

Travel utilities were measured in savings, totaling 98.8 USD/day for the entire settlement with 28% less CO_2 emissions by 2030. Considering the time frame (2019–2030), if the model were applied after the 2010 Mt. Merapi eruptions, with an operational expense of 18.36 USD per motorcycle (Herwangi et al. 2017), then 2.39 VKT/person/day would save 105.6 USD from daily travel expenses incurred by all HHs in 2019. Mobility profiles show an approximate 2:1 ratio for motorcycles (68%) and walking modes (32%). Consequently, travel expenditures fell to 18.4% of the average monthly income with 6 USD savings per person as seen in Table 8.

The interpolation of results reveals their extent (urban form data in Supplementary Table S10):

- Access to 3.5 times more transit volume and a 32% pedestrian mode shift rendered a suitable environment for livelihood diversification.
- People over 50-years-old with upper median incomes and risk-taking behaviors had the highest probability of venturing a home business.
- Land-use treatment in nodes had a direct effect on land-use change between the nodes. The model satisfied 56% of the housing demand, leading to mixed-use development.
- The residential allocation model revealed that HHs sought locations close to valued destinations in low-density areas with a negative correlation to vacancy.
- Allocation of HHs with individual attributes reduced intra-settlement travel distance by half. This had a strong effect on agents shifting from vehicle to walking modes (22%).
- The OLUTM model demonstrates that people utilized 21%–26% of their monthly income before the intervention and 11%–18.4% after with a modest bus service (Supplementary Fig. S10). Monthly travel savings amount to 3,172 USD (2019) and 3,636 USD (2030).

6.1. Limitations and assumptions

A series of constraints were met. For example, clustering with occupational profiles was insufficient due to the scale of the settlement having a small number of HHs. Simplifications follow the prospect theory for utility-based decisions, but the assumptions in Table 9 entail further research. The data collected represents a portion of the ideal amount for microscopic simulation. Furthermore, large datasets are not easily found for rural areas.

6.2. Conclusions

This study provides a detailed description of the OLUTM model to evaluate post-disaster mobility, aiming to clarify whether a land-use network with distributed livelihood options can complement rural labor in a recovery scenario. The outcome revealed a substantial reduction of travel expenses with an agronomic-centric network. Livelihood diversification is predicted based on sociodemographic data and local employment structures influencing a broad spectrum of job opportunities. As a result, 94 livelihood diversifications were recorded in the simulation with 63% accounting for farmers. Findings suggest that they are risk-oriented individuals with incomes above the average. Together with travel utility savings, the AUB network secured farming as the primary employment and HBEs as the secondary employment.

While the expected development of an AUB network provides travel efficiency and access to opportunities, resettlement offers a chance to locate HHs that will potentially venture micro-industries, known to be compatible with agriculture in the region. AUB networks are envisioned to accommodate public transport on existent roads to avoid further rural fragmentation. However, incentives are required to promote intensive agriculture in contiguous parcels and deaccelerate extensive agricultural land-use conversion. These policies should reinforce dairy cooperatives with agronomic business training to avoid large real estate transactions. There is also a need for land-use planning and hazard mitigation infrastructure. Together with forest protection policies, tree farming could become a source of labor for paper, wood, and biopolymer industries which could help to absorb future hazard shocks. AUB networks also target resource depletion with rural labor, land cover, energy-efficient travel, and semi-urban development to reduce urban intensities and enclose that growth in city-wide areas. This is especially important for Yogyakarta and the environmental stability of its surroundings.

Future research is directed towards the effect of relocation on human dynamics and a site-selection model for the Geographic Environment. The OLUTM model represents a continued effort to address urban growth and develop land use-transportation policy. Although the model is not yet operational, the results reported here document a major step in our agenda.

Declaration of Competing Interest

The authors declare that they have no known competing financial interests or personal relationships that could have appeared to influence the work reported in this paper.

Acknowledgements

The corresponding author is in great debt of appreciation to the Japanese Ministry of Education, Culture, Sports, Science, and Technology for supporting this research. The authors extend their sincere gratitude to the reviewers and editors of this journal for the crucial guidance throughout the review process. We would also like to thank Rachmad Wirawan for his assistance in surveying the study area and Gabriela Wurst for the unconditional support revising the manuscript.

This research received no external funding.

Appendix A. Supplementary material

Supplementary data to this article can be found online at https://doi.org/10.1016/j.trd.2022.103189.

References

Alkhresheh, M.M., 2007. Enclosure as a Function of Height-to-Width Ratio and Scale: Its Influence on User's Sense of Comfort and Safety in Urban Street Space. University of Florida, Gainesville, FL https://ufdc.ufl.edu/UFE0019676/00001.

Alonso, W., 2013. Location and Land Use: Toward a General Theory of Land Rent. Harvard University Press, Cambridge, MA and London. Accessed: August, 2019. http://dx.doi.org/10.4159/harvard.9780674730854.

Arlinghaus, S.L., Arlinghaus, W.C., Harary, F., 2002. Graph Theory and Geography: An Interactive View (Ebook). Wiley and Sons, New York http://hdl.handle.net/2027.42/58623.

Bartik, T.J., 1991. Who Benefits from State and Local Economic Development Policies?, W.E. Upjohn Institute Press, Michigan, 354 pp. https://www.jstor.org/stable/j.ctvh4zh1q.

Bowman, J.L., Ben-Akiva, M.E., 2001. Activity-based disaggregate travel demand model system with activity schedules. Transp. Res. Part A: Policy Pract. 35 (1), 1–28. https://doi.org/10.1016/S0965-8564(99)00043-9.

Bray, F., 1994. Agriculture for Developing Nations. Scientific America. https://www.academia.edu/35944993/Agriculture_for_Developing_Nations.

Chapin, F.S., 1974. Human activity patterns in the city: Things people do in time and in space, Wiley- Interscience, New York, 507 pp. https://www.abebooks.com/9780471145639/Human-activity-patterns-city-Things-0471145637/plp.

Charpe, M., 2019. Sectoral Employment Multipliers in Rwanda: Comparing local multipliers and input-output analysis. Int. Labor Org.-Geneva, 1-26. https://www.ilo.org/wcmsp5/groups/public/—ed_emp/—ifp_skills/documents/publication/wcms_723283.pdf.

Clifton, K., Ewing, R., Knaap, G., Song, Y., 2008. Quantitative analysis of urban form: A multidisciplinary review. J. Urbanism: Int. Res. Placemaking Urban Sust. 1 (1), 17–45. https://doi.org/10.1080/17549170801903496.

Contreras, D., Blaschke, T., Hodgson, M.E., 2017. Lack of spatial resilience in a recovery process: Case L'Aquila Italy. Tech. Forecast. Soc. Change 121, 76–88. https://doi.org/10.1016/j.techfore.2016.12.010.

Dancer, S., 2015. Employment Densities Guide, 3rd. ed. Government UK: Homes and Communities Agency, 1-40. https://www.kirklees.gov.uk/beta/planning-policy/pdf/examination/national-evidence/NE48_employment_density_guide_3rd_edition.pdf.

Garcia-Fry, M., Murao, O., 2020. A Post-Disaster Forecast Analysis for Relocation Settlements using a Combined Model Sequence, 17th World Conf. on Earthq. Eng: N. C000108, Sendai, 1–12. https://www.researchgate.net/publication/344756575_A_POSTDISASTER_FORECAST_ANALYSIS_FOR_RELOCATION_SETTLEMENTS_USING_A_COMBINED_MODEL_SEQUENCE.

[Dataset 1] Garcia-Fry, M., 2021. OLUTM Model Dataset. Mendeley Data, v3. http://dx.doi.org/10.17632/t9p23k3pyn.3.

Gaughan, A.E., Stevens, F.R., Linard, C., Jia, P., Tatem, A.J., 2013. High Resolution Population Distribution Maps for Southeast Asia in 2010 and 2015. PLoS ONE 8 (2), e55882. https://doi.org/10.1371/journal.pone.0055882.

Giyarsih, S.R., 2010. Urban Sprawl of the City of Yogyakarta, Special Reference to the Stage of Spatial Transformation (Case Study at Maguwoharjo Village, Sleman District). Indonesian J. Geog. 42 (1), 47–58. https://jurnal.ugm.ac.id/ijg/article/view/1576.

Hägerstraand, T., 1970. What about People in Regional Science? Papers Reg. Sci. 24 (1), 7–24. https://doi.org/10.1111/j.1435-5597.1970.tb01464.x.

Han, B., Sun, D., Yu, X., Song, W., Ding, L., 2020. Classification of Urban Street Networks Based on Tree-Like Network Features. Sustainability 12 (2), 628–641. https://doi.org/10.3390/su12020628.

Handy, S.L., Boarnet, M.G., Ewing, R., Killingsworth, R.E., 2002. How the built environment affects physical activity. Am. J. Prev. Med. 23 (2), 64–73. https://doi.org/10.1016/S0749-3797(02)00475-0.

Herwangi, Y., Pradono, P., Syabri, I., Kustiwan, I., 2017. Transport Affordability and Motorcycle Ownership in Low–income Households: Case of Yogyakarta Urbanised Area, Indonesia, Proceedings of the Eastern Asia Society for Transportation Studies 12th conference. Ho Chi Minh, Vietnam. https://pdfs.semanticscholar.org/cc76/3d8152d8b58434732d7b6ca9df8c4a559580.pdf?_ga=2.180259811.67623511.1589852803–1018558182.1589195121.

Hynynen, A., 2006. Node-Place-Model-A strategic tool for regional land use planning. Nordisk arkitekturforskning -. Nordic J. Arch. Res. 18 (4), 21–29. http://arkitekturforskning.net/na/article/view/164.

[Dataset 2] Indonesia, Statistics of D.I. Yogyakarta Province, 2020. Delivering Data to Inform Development Planning. Division of Integrated Data Processing and Statistical Dissemination, Catalog: 1102002.34, pp. xxiv–552. Accessed: April, 2020. https://yogyakarta.bps.go.id/publication/2020/02/28/b734b0efb96248fa39801969/provinsi-di-yogyakarta-dalam-angka-2020–penyediaan-data-untuk-perencanaan-pembangunan.html.

[Dataset 3] Indonesia, Statistics Sleman Regency, 2018. Population and Population Growth Rate by Subdistrict in Sleman Regency, 2010, 2016, and 2017. Badan Pusat Statistik Kabupaten Sleman. Accessed: May 19, 2020. https://slemankab.bps.go.id/statictable/2018/10/12/363/jumlah–penduduk–dan–laju–pertumbuhan–penduduk–menurut–kecamatan–di–kabupaten–sleman–2010–2016–dan–2017.html.

[Dataset 4] Indonesia, Statistics of D.I. Yogyakarta Province, 2019. Population Distribution and Density by Subdistrict in Sleman Regency, 2018", Badan Pusat Statistik Kabupaten Sleman. Accessed: Oct. 25, 2021. https://slemankab.bps.go.id/statictable/2019/07/09/520/distribusi-dan-kepadatan-penduduk-menurut-kecamatan-di-kabupaten-sleman-2018.html.

Jones, P.M., 1977. New Approaches to Understanding Travel Behaviour: The Human Activity Approach, Working Paper 28, Transp, Stud. Unit, University of Oxford, Oxford, England.

Kahneman, D., Tversky, A., 1979. Prospect theory: An analysis of decision under risk. Econometrica 47 (2), 263–292. https://doi.org/10.2307/1914185.

Kitamura, R., 2009. Life-style and travel demand. Transp. 36, 679–710. https://doi.org/10.1007/s11116-009-9244-6.

Krizek, K.J., 2003. Operationalizing Neighborhood Accessibility for Land Use-Travel Behavior Research and Regional Modeling. J. Plan. Edu. Res. 22 (3), 270–287. https://doi.org/10.1177/0739456X02250315.

Lauf, S., Haase, D., Seppelt, R., Schwarz, N., 2012. Simulating Demography and Housing Demand in an Urban Region under Scenarios of Growth and Shrinkage. Environ. Plan. B Plan. Des. 39 (2), 229–246. https://doi.org/10.1068/b36046t.

Levinson, D.M., Wu, H., 2020. Towards a general theory of access. J. Transp. Land Use 13 (1), 129–158. https://doi.org/10.5198/jtlu.2020.1660.

Linard, C., Gilbert, M., Tatem, A.J., 2011. Assessing the use of global land cover data for guiding large area population distribution modelling. GeoJournal 76, 525–538. https://doi.org/10.1007/s10708-010-9364-8.

Litman, T., 2021. Evaluating Accessibility for Transport Planning. Victoria Transp. Policy Inst. 1–62. https://www.vtpi.org/access.pdf.

Maly, E., Iuchi, K., Nareswari, A., 2015. Community-Based Housing Reconstruction and Relocation: Rekompak Program after the 2010 Eruption of Mt. Merapi Indonesia. J. Soc. Safety Sci. 27, 205–214. https://doi.org/10.11314/jisss.27.205.

McCamant, K., Durret, C., Hertzman, E., 1994. Cohousing: A Contemporary Approach to Housing Ourselves, 2nd Edition. ed. Ten Speed Press, Berkeley.

MDA Federal Inc. (1995–2007) EarthSat GeoCover LC Overview. Rockville, MD: MacDonald, Dettwiler, and Associates Ltd. Available: http://www.mdafederal.com/geocover/geocoverlc/gclcoverview.

Mennis, J., Hultgren, T., 2006. Intelligent Dasymetric Mapping and Its Application to Areal Interpolation. Cartogr. Geog. Inf. Sci. 33 (3), 179–194. https://doi.org/10.1559/152304006779077309.

Meszler, D., 2007. Emissions Issues Related to Two–and Three–Wheeled Motor Vehicles. Meszler Engineering Services, pp. 20–24. Accessed: April 2020. https://theicct.org/sites/default/files/publications/twothree_wheelers_2007.pdf.

Miller, M.A., 2018. Reconfiguring rural aspirations through urban resettlement: Navigating futurity after the 2010 eruption of Mount Merapi, Indonesia. In: Bunnell, T., and Goh, D., (Ed.), Urban Asias: Essays on Futurity Past and Present, Jovis, Berlin, pp. 193–202. https://urbanaspirationsasia.com/urban-asias/.

Miller, E.J., 2018. The case for microsimulation frameworks for integrated urban models. J. Transp. Land Use 11 (1), 1025–1037. https://doi.org/10.5198/jtlu.2018.1257.

Miller, E.J., and P.A., Salvini., (2005). ILUTE: An Operational Prototype of a Comprehensive Microsimulation Model of Urban Systems. Netw. Spat. Econ. 5, 217–234. https://doi.org/10.1007/s11067-005-2630-5.

Millonig, A., Schechtner, K., 2007. Developing Landmark-Based Pedestrian-Navigation Systems. IEEE Trans. Intell. Transport. Syst. 8 (1), 43–49. https://doi.org/10.1109/TITS.2006.889439.

Moeckel, R., Wegener, M., Spiekermann, K., 2003. Creating a Synthetic Population. In: In: 8th International Conference on Computers in Urban Planning and Urban Management (CUPUM), pp. 1–18.

Mohammadi, N., Taylor, J.E., 2019. Recurrent Mobility: Urban Conduits for Diffusion of Energy Efficiency. Sci. Rep. 9 (20247), 1–12. https://doi.org/10.1038/s41598-019-56372-4.

Moretti, E., 2010. Local Multipliers. Amer. Econ. Rev: Papers Proc. 100 (2), 1–7. https://eml.berkeley.edu/~moretti/multipliers.pdf.

Nystuen, J.D., Dacey, M.F., 2005. A Graph Theory Interpretation of Nodal Regions. Papers Reg. Sci. 7, 29–42. https://doi.org/10.1111/j.1435-5597.1961.tb01769.x.

OSM-OpenStreetMap, 2021. The Free Wiki World Map. Open-Street Map contributors, CC BY-SA. Accessed April 15, 2021. Available: http://www.openstreetmap.org/ [Internet].

Peponis, J., Bafna, S., Zhang, Z., 2008. The Connectivity of Streets: Reach and Directional Distance. Environ. Plan. B: Plan. Des. 35 (5), 881–901. https://doi.org/10.1068/b33088.

Pramana, A.Y.E., 2016. Impact of Land Use Regulation on Land Values. Erasmus University, Rotterdam, 61 pp. http://hdl.handle.net/2105/42298.

Rondhi, M., Pratiwi, P.A., Handini, V.T., Sunartomo, A.F., Budiman, S.A., 2018. Agricultural Land Conversion, Land Economic Value, and Sustainable Agriculture: A Case Study in East Java Indonesia. Land 7 (4), 148–167. https://doi.org/10.3390/land7040148.

Rijanta, R., 2008. Livelihood Strategies, Responses to the Crisis, and the Role of Non-Agricultural Activities in Five Villages in the Special Region of the Yogyakarta. In: Titus, M.J., Burgers, P.P.M. (Eds.), Rural Livelihoods, Resources and Coping with Crisis in Indonesia: A Comparative Study. ICAS Publication Series, Amsterdam University Press, Amsterdam, p. 155.

Rijanta, R., 2009. Determinants to Rural Diversification in Java, Indonesia: The Case of Yogyakarta Special Province (DIY). Reg. Views 22, 1–15. https://www.researchgate.net/publication/272941622_Determinants_to_Rural_Diversification_in_Java_Indonesia_the_Case_of_Yogyakarta_Special_Province_DIY.

Rindrasih, E., 2018. Under the Volcano: Responses of a Community-Based Tourism Village to the 2010 Eruption of Mount Merapi Indonesia. Sustainability 10 (5), 1–17. https://doi.org/10.3390/su10051620.

Rudlin, D., Falk, N., 1999. Building the 21st Century Home: The Sustainable Urban Neighborhood. Architectural Press, Oxford, pp. 215–217.

Singgih, B.A., Asano, J., 2019. Study on Impact of Relocating Settlement as a Post-Disaster Mitigation. Urb. Reg. Plan. Rev. 6, 111–124. https://doi.org/10.14398/urpr.6.111.

Sleman Regency, 2012. Rencana Tata Ruang Wilayah Kabupaten Sleman Tahun 2011-2031, The Sleman Regency of Yogyakarta DIY. https://peraturan.bpk.go.id/Home/Details/35750 (Accessed 15 May 2020).

Stevens, F.R., Gaughan, A.E., Linard, C., Tatem, A.J., 2015. Disaggregating Census Data for Population Mapping Using Random Forests with Remotely-Sensed and Ancillary Data. PLoS ONE 10 (2), e0107042. https://doi.org/10.1371/journal.pone.0107042.

Sugiyanto, G., 2016. The Effect of Congestion Pricing Scheme on the Generalized Cost and Speed of a Motorcycle. Walailak J. Sci. Tech. (WJST) 15 (1), 95–106. https://doi.org/10.48048/wjst.2018.2347.

Sun, B., Robinson, D.T., 2018. Comparison of Statistical Approaches for Modelling Land-Use Change. Land 7 (4), 144–177. https://doi.org/10.3390/land7040144.

The World Bank, 2016. Community-based Settlement Rehabilitation and Reconstruction Project for Central and West Java and Yogyakarta Special Region. Report No: ICR00003662, pp. 5-25. https://documents1.worldbank.org/curated/en/655251467992043861/text/ICR3662-P103457-OUO-9.txt.

The World Bank, 2012. REKOMPAK; Rebuilding Indonesia's Communities After Disasters [WWW Document]. Financial Literacy and Education Russia Trust Fund, pp. 43-44. Accessed January, 2019. https://documents.worldbank.org/en/publication/documents-reports/documentdetail/128361468267347740/rekompak-rebuilding-indonesias-communities-after-disasters.

Tutuko, P., 2014. Residential Land Use and Housing Development in Indonesia from the Perspective of Sustainable Urban Form, Thesis Abstract, Graduate School of Natural Science and Technology, Division of Environmental Science and Engineering, Kanazawa University. http://hdl.handle.net/2297/40520.

Umaya, R., Hardjanto, Soekmadi, R., Sunito, S., 2020. Livelihood adaptation patterns of sub-villages communities in the slope of Merapi Volcano. IOP Conf. Ser: Earth Environ. Sci. 528, p. 1. https://doi.org/10.1088/1755-1315/528/1/012020.

Waddell, P., Borning, A., Noth., M., Freier, N., Becke, M., Ulfarsson, G., 2003. Microsimulation of Urban Development and Location Choices: Design and Implementation of UrbanSim. Netw. Spat. Econ. 3, 43–67. https://doi.org/10.1023/A:1022049000877.

Wagner, P., Wegener, M., 2007. Urban Land Use, Transport and Environment Models. disP - Plan. Rev. 43 (170), 45–56. https://doi.org/10.1080/02513625.2007.10556988.

Wegener, M., Fuerst, F., 2004. Land-Use Transport Interaction: State of the Art. Integration of Transport and Land Use Planning (TRANSLAND) 2A. SSRN Electronic J. 1–119. https://doi.org/10.2139/ssrn.1434678.

Widowaty, Y., Oktavian Artanto, I., 2018. In: Protection of Agricultural Land Sustainable Food for the Realization of Food Security in The Special Region of Yogyakarta. Atlantis Press, Paris, pp. 35–40. https://doi.org/10.2991/fanres-18.2018.8.

Yang, Y., Diez-Roux, A. v., 2012. Walking Distance by Trip Purpose and Population Subgroups. Am. J. Prev. Med. 43(1), 11–19. https://doi.org/10.1016/j.amepre.2012.03.015.

Yokohari, M., 2006. Agro-activities in the Fringe of Asian Mega-Cities. Landsc. Ecol. Manag. 10 (2), 75–79. https://doi.org/10.5738/jale.10.75.

Zhu, Y., Diao, M., Ferreira, J., Zegras, C., 2018. An integrated microsimulation approach to land-use and mobility modeling. J. Transp. Land Use 11 (1), 663–1659. https://doi.org/10.5198/jtlu.2018.1186.

Zondag, B., de Bok, M., Geurs, K.T., Molenwijk, E., 2015. Accessibility modeling and evaluation: The TIGRIS XL land-use and transport interaction model for the Netherlands. Comp. Environ. Urb. Syst. 49, 115–125. https://doi.org/10.1016/j.compenvurbsys.2014.06.001.

Glossary

Acronym: Definition
HH: Households
OLUTM: Operational land use and transport microsimulation
USD: United States Dollars
HBEs: Home Business Entrepreneurships
m^2: Square–meters
km: Kilometers
TAZ: Traffic analysis zone
VKT: Vehicle kilometers travelled
CO_2: Carbon dioxide
APH: Adults per household
RTRW: Rencan Tata Ruang Wilayah
Lp: Low performance
Hp: High performance
m: Meters
H:W: Height to width
Ha: Hectares
AUB: Agronomic urban boundary
OSM: Open street map
GIS: Geographic information systems
GEE: Google Earth Engine
RDW: Residential demand weight